Journal of Nuclear Materials 390–391 (2009) 482–485

Contents lists available at ScienceDirect

Journal of Nuclear Materials

journal homepage: www.elsevier.com/locate/jnucmat

Spatially resolved charge exchange flux calculations on the Toroidal Pumped Limiter of Tore Supra

Y. Marandet [a,*], E. Tsitrone [b], P. Börner [c], D. Reiter [c], A. Beauté [b], E. Delchambre [b], A. Escarguel [a], S. Brezinsek [c], P. Genesio [a], J. Gunn [b], P. Monier-Garbet [b], R. Mitteau [b], B. Pégourié [b]

[a] PIIM, CNRS/Université de Provence, Marseille, France
[b] Association Euratom-CEA, CEA/DSM/DRFC CEA Cadarache, France
[c] IEF-4 Plasmaphysik, Forschungszentrum Juelich GmbH, Association EURATOM-FZJ, TEC, Germany

ARTICLE INFO

PACS:
52.25.Ya
52.40.hf
52.60.Pp
52.25.Vy

ABSTRACT

A spatially resolved calculation of the charge exchange particle and energy fluxes on the Toroidal Pumped Limiter (TPL) of Tore Supra is presented, as a first step towards a better understanding and modelling of carbon erosion, migration, as well as deuterium codeposition and bulk diffusion of deuterium in Tore Supra. The results are obtained with the EIRENE code run in a 3D geometry. Physical and chemical erosion maps on the TPL are calculated, and the contribution of neutrals to erosion, especially in the self-shadowed area, is calculated.

1. Introduction

Mitigating tritium retention is one of the major challenges that need to be addressed to achieve successful operation of ITER and other future fusion devices. The deuterium inventory in Tore Supra (DITS) campaign carried out this year was aimed at a better understanding of deuterium retention mechanisms [1]. One of the ingredients to be analysed in this campaign is the contribution of charge exchange neutrals to the incident particle flux to the wall. Indeed, the latter contributes to bulk diffusion and codeposition through wall erosion. Previous work relied on EIRENE [2] calculations in a 2D geometry and has provided the poloidal distribution of the charge exchange neutrals (CX) flux and its energy spectrum [3]. However, the flux pattern on the Toroidal Pumped Limiter (TPL) is highly inhomogeneous [4], and the resulting erosion/deposition pattern with thick and thin deposits in the vicinity of net erosion zones calls for a spatially resolved calculation along the toroidal direction. We model here this complex environment using EIRENE in a 3D toroidal geometry. In particular, chemical erosion on the TPL should be estimated as accurately as possible, as a first step towards carbon erosion and deposition modelling. Furthermore, radiative heating of the deposits enhances chemical sputtering by CX atoms in the deposition area. This has recently been highlighted [5] as a possible mechanism responsible for carbon migration. The paper is organized as follows. We first describe the simulations set-up, then present the results about the CX flux maps and finally discuss physical and chemical sputtering on the TPL.

2. Description of the simulations

The EIRENE calculations presented here rely on an extension of the simplified 2D geometry used previously to a 3D toroidal geometry, where 20° of the torus are simulated (in the toroidal direction), with 64 toroidal cells. This 20° corresponds to the spacing between coils, and toroidal periodicity is assumed at the end of the simulation domain. Using a 3D geometry has two major advantages. First of all, the complex D^+ particle flux pattern induced by magnetic ripple on the TPL [4] can be taken into account (Fig. 1). In particular, there are self-shadowed zones where magnetic field lines are connected to the TPL over very short distances (connection length smaller than 1 m), and which behave like private flux zones (see Ref. [4] for a cartoon). The latter are however not shielded from the CX flux. In the 3D geometry, charge exchange (CX) flux maps on the TPL (in particular in the self-shadowed area), as well as sputtering maps can be calculated. Secondly, direct comparison to spectroscopic diagnostics will be possible. The spatially fully resolved incoming flux distribution on the limiter is reconstructed from reciprocating Langmuir probe measurements, using the 3D magnetic configuration including ripple and the Shafranov shift [4]. The radial particle flux Γ decay in the SOL is approximated by an exponential function with a characteristic length $\lambda_p = 3$ cm. Its value Γ_0 at the last closed flux surface, i.e. the recycling flux, is determined by scaling the total D^+ flux on the TPL using a 0D balance model, the parameters of which are calculated with EIRENE. For the discharges considered here, this model gives $\Gamma_{D+} = 10^{22}$ part s^{-1}, of which roughly 85% falls on the TPL roof. Adding a 10% fraction of perpendicular flux is necessary to explain the temperature pattern measured by the IR camera in the region

* Corresponding author.
E-mail address: yannick.marandet@piim.up.univ-mrs.fr (Y. Marandet).

0022-3115/$ - see front matter © 2009 Elsevier B.V. All rights reserved.
doi:10.1016/j.jnucmat.2009.01.050

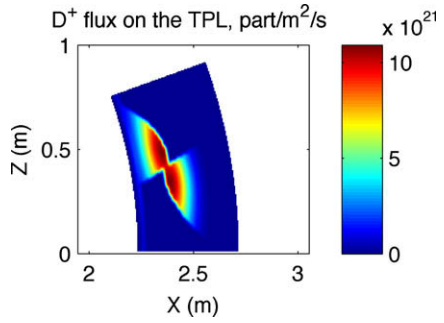

Fig. 1. Input D+ particle flux pattern on the TPL (view from the top of the torus, 20° in the toroidal direction), in part m^{-2} s^{-1}. The complex pattern results from magnetic ripple.

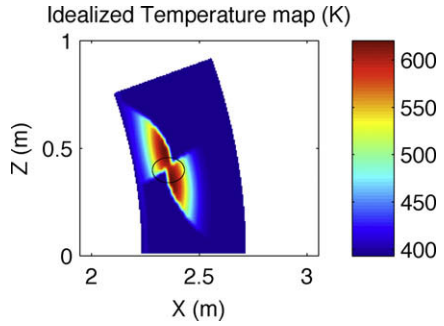

Fig. 2. Idealized temperature map on the TPL (K). The black ellipse shows the region of tangency of the magnetic field lines on the TPL, where perpendicular flux dominates.

where field lines have grazing incidence on the TPL and the contribution of the parallel flux becomes negligible [6] (see Fig. 2, where this region is indicated by an ellipse). In the self-shadowed regions, the ion flux is defaulted to 0, since the corresponding decay lengths in the SOL are very short. The spatial D^+ flux map on the TPL roof thus obtained is used in EIRENE to sample D^+ ions hitting the surface, and then recycling them as atoms or molecules. The ion flux flowing beyond 4.5 cm in the SOL, which falls on the neutralisers below the TPL, and amounts to 15% of the total flux, is also included in the simulation, but without toroidal resolution. An idealized (in the sense that deposits are ignored as a first step) surface temperature map on the actively cooled TPL roof is also taken into account (Fig. 2), and is obtained using the formula $T_{surf}(°C) = 120 + 80^{*}\varphi_q(MW)$ (which is deduced from thermo-mechanical calculations [6]) where φ_q is the heat flux. Background plasma parameters are reconstructed from measurements, and their consistency is checked from power balance. They correspond to the Tore Supra long discharge scenario used in [3], where $n_e(0) = 2.2 \times 10^{19}$ m^{-3}, $n_e(a) = 4 \times 10^{18}$ m^{-3}, $T_e(0) = 3.8$ keV and $T_e(a) = 90$ eV where 0 stands for the centre and a for the last closed flux surface. The central ion temperature is not measured and its value ($T_i(0) = 2$ keV) is deduced from power balance, while consistency of the latter in the edge requires $T_i = 2T_e$ for this scenario. For the moment, this plasma background is taken to be toroidally homogeneous.

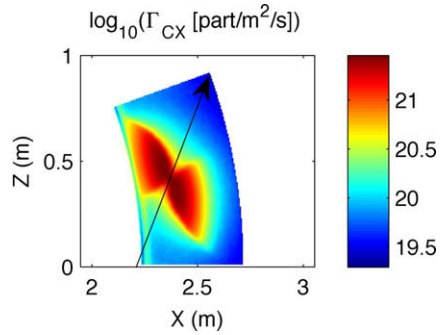

Fig. 3. Charge exchange flux map on the TPL (log scale), in part m^{-2} s^{-1}. The flux in the shadowed area is significant. The solid arrow indicates the direction along which the profiles of Fig. 4 are plotted. Its direction is such that it measures the distance in the shadowed area.

3. Charge exchange flux

The total CX flux onto the TPL obtained from the simulations is $\Gamma_{D0}^{TPL} = 3.2 \times 10^{21}$ part s^{-1}, that is roughly 35% of the incoming D^+ flux. On the First Wall (FW), we have $\Gamma_{D0}^{FW} = 2.9 \times 10^{21}$ part s^{-1}, showing that in this case the CX flux on the TPL roof is of the same order as on the first wall. These results show a reasonable agreement with previous 2D results (when comparing to the results of Ref. [3], it should be noted that the recycling coefficient is set to one in the current simulations, since the flux pumped by the wall is negligible compared to the recycling flux, namely 2×10^{20} part s^{-1} versus 10^{22} part s^{-1}), and the interpretation of the slightly lower fluxes obtained on the first wall in the 3D case is difficult. In fact, the ion flux flowing deeper than 4.5 cm in the SOL gives a significant contribution to the first wall, and its treatment is only approximate here. An improved calculation would require launching ions in a reconstructed 3D magnetic field, and this will be the subject of a future work. However, this is not a serious issue here, since it only globally rescales the total ion flux falling on the TPL roof. Let us now focus on the spatial pattern of the CX flux on the TPL, plotted in log scale in Fig. 3. Its spatial distribution is clearly similar to that of the incoming D^+ flux, but smeared out on a scale of the order of the neutral mean free path (~10 cm). Fifteen percent of this flux falls into the self-shadowed area, with a decay length of the order of 10 cm (see Fig 4, where the CX flux profile is plotted along the arrow indicated in Fig. 3). Consequences in terms of sputtering are studied in the next section. The CX energy flux in the self-shadowed area has a maximum of the order of 0.05 MW/m^2 for the scenario considered here. The decay length is again found to be of 10 cm. This has to be compared to peak radiation fluxes of the order of 0.03–0.3 MW/m^2 in [5]. The spatial distributions are however significantly different. In fact, radiation fluxes have a larger decay length, so that deposits far away (toroidally) in the self-shadowed area are probably mainly radiation heated. However, further investigations are needed since this conclusion depends on discharge scenarios, and carbon concentration in the plasma.

4. Physical and chemical sputtering map on the toroidal pumped limiter

Physical sputtering is calculated here using the revised Bohdansky formula [7] .The total carbon flux eroded by physical sputtering on the TPL is $\Gamma_C^{phys} = 2.7 \times 10^{20}$ part s^{-1}, which corresponds to a global sputtering rate of roughly $Y_{phys} \sim 2\%$. Comparison to an estimate taking only the ion flux into account shows that neutrals are responsible for about 25% of this carbon flux. The contribution of the self-shadowed areas of the TPL to Γ_C^{phys} is 1.4×10^{19} part s^{-1}, so that only 5% of physical sputtering takes place in these regions. It is nevertheless clearly visible in Fig. 5, which is plotted on log scale. Self-sputtering gives a contribution of the same order as physical sputtering in the conditions considered here [5]. The chemical sputtering map is calculated using the idealized temper-

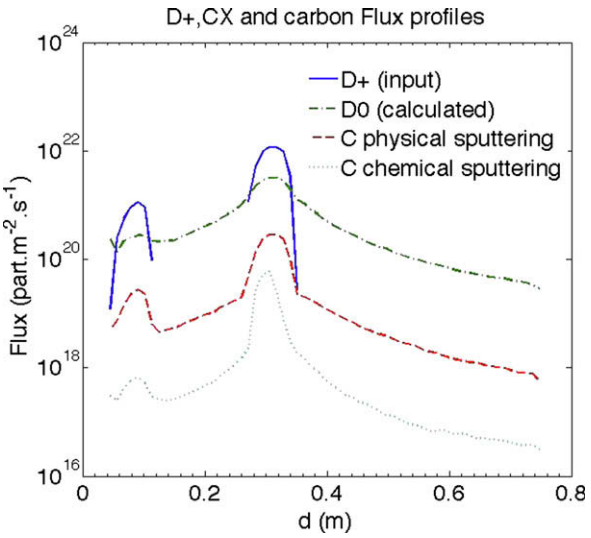

Fig. 4. Ion, CX and carbon fluxes profiles along the solid arrow plotted on Fig. 3. The decay length for the CX fluxes and the associated carbon erosion is of the order of 10 cm. The peak centred around $d = 0.1$ m corresponds to the leading edge.

ature map of Fig. 2, and is plotted in Fig. 6. The flux used to calculate the sputtering yield with Roth's formula [8] is the total flux ($\Gamma = \Gamma_{D+} + \Gamma_{D0}$, where the CX flux Γ_{D0} has to be computed in a first iteration). The total chemically eroded carbon flux amounts to $\Gamma_C^{chem} = 2.4 \times 10^{19}$ part s^{-1}, and the contribution of the self-shadowed area is 7×10^{17} part s^{-1}, i.e. only 3% of the total chemically eroded carbon. The average chemical sputtering yield on the TPL is therefore found to be $Y_{chem} \sim 0.2\%$, while spectroscopy typically gives $Y_{chem} \sim 1$–2% in Tore Supra [9]. The simulated values are found to be lower than the experimental ones by an order of magnitude. The low value of Y_{chem} obtained in the simulations (0.2%) primarily results from the low surface temperature of the TPL (see Fig. 2), which is actively cooled. In fact, depending on the flux, the maximum of the chemical erosion yield Y_{chem} shifts from 700 to 1000 K as the flux increases, and Y_{chem} sharply drops for temperatures lower than this maximum [7]. However, this steep decrease does not seem to be universally observed, e.g. [10] for TEXTOR measurements, a fact that might explain the differences between calculations and measurements. Another source of discrepancy is related to the fact that, at the present stage, deposits, especially in the gaps between tiles in the plasma wetted area, are not explicitly taken into account. The existence of deposits has at least two effects as far as the treatment of chemical erosion is concerned. First, their temperature is much higher than that expected from the simple formula used here because of poor thermal contact with

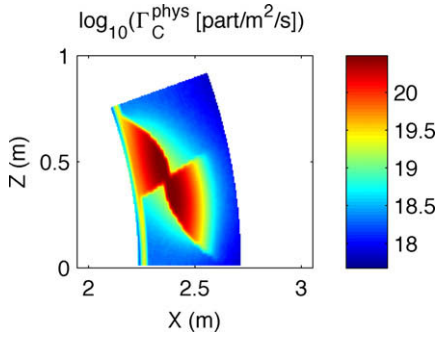

Fig. 5. Physical sputtering map in log scale, including ion and CX contribution. Erosion by the CX flux is clearly visible, but is rather low.

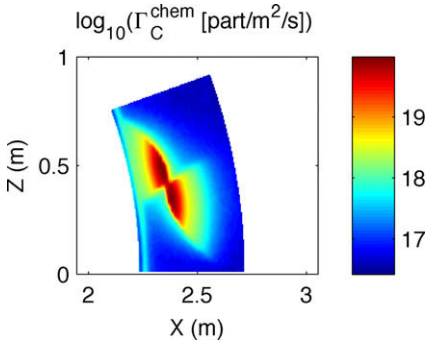

Fig. 6. Chemical sputtering map in log scale, obtained from application of Roth's formula, including ion and CX contribution.

the bulk of the limiter. In fact, the possible role of gap deposits has already been highlighted in simulations carried out with the BBQ code [5], and is potentially important because they are formed in a region where the flux is high. This temperature effect is certainly also significant in the zone of tangency of the magnetic field lines on the TPL, delimited by the ellipse in Fig. 2, which shows a high temperature on the IR camera (typically 700–800 K). Next, laboratory measurements [11] and analysis of Quartz Micro Balance data with the ERO code [12] have shown that Y_{chem} is higher by a factor of up to more than 100 on redeposited layers (depending on their D/C ratio) than on pure graphite. As a result, even though Roth's formula pertains to a mixture of several carbon surface states, when the latter is used locally on deposits a correction factor should be applied. The contribution of the self-shadowed area can thus be roughly estimated to be 7×10^{18} part s^{-1}, assuming it is covered 100% by deposits having the same properties (i.e. a factor 10 increase in Y_{chem}). If the average temperature in this zone is taken to be 600 K (instead of ~400 K), the contribution of the self-shadowed area further increases to 3.5×10^{19} part s^{-1}. As proposed in [5], chemical erosion by the CX flux of radiatively heated deposits in the self-shadowed area might therefore be an efficient drive for carbon migration, in spite of being a rather small overall carbon source.

5. Conclusions

The total charge exchange flux on the TPL corresponds to 35% of the incoming ion flux, for the scenario studied here. This result is consistent with previous 2D calculations. The proportion of this flux falling in the self-shadowed area is 15% with a characteristic decay length of the order of 10 cm. The contribution of CX neutrals to physical sputtering is about 25%. The calculations remain preliminary for chemical erosion, and most probably significantly underestimate the latter ($Y_{chem} \sim 0.2\%$). This might be related to deviations from Roth's formula at low surface temperature (400–500 K). Chemical sputtering by the CX flux of mainly radiatively heated deposits in the self-shadowed regions is confirmed as a possibly efficient drive for carbon migration. An improved estimation taking into account the localisation of deposits and their temperature on the limiter will be carried out. Detailed comparison to spectroscopic measurements is currently ongoing.

Acknowledgements

Enlightening discussions with A. Kirchner and D. Borodin are gratefully acknowledged. This work is part of a collaboration (LRC DSM 99-14) between the laboratoire PIIM (UMR 6633) and the IRFM, CEA Cadarache, in the frame of the Fédération de Recherche sur la Fusion Magnétique (FRFM).

References

[1] B. Pégourié et al., J. Nucl. Mater. 390–391 (2009) 550.
[2] Reiter, M. Baelmans, P. Börner, Fusion Sci. Technol. 47 (2005) 172.
[3] E. Tsitrone et al., J. Nucl. Mater. 337–339 (2005) 539.
[4] R. Mitteau et al., J. Nucl. Mater. 266–269 (1999) 798.
[5] J. Hogan et al., J. Nucl. Mater. 363–365 (2007) 167.
[6] R. Mitteau et al., J. Nucl. Mater. 313–316 (2003) 1229.
[7] W. Eckstein et al., IPP report 9/117, Garching, 1993.
[8] J. Roth et al., Nucl. Fusion 44 (2004) L21.
[9] E. Delchambre et al., J. Nucl. Mater. 390–391 (2009) 65.
[10] S. Brezinsek et al., J. Nucl. Mater. 363–365 (2007) 1119.
[11] A. Von Keudell et al., Nucl. Fusion 39 (1999) 1451.
[12] A. Kirschner et al., J. Nucl. Mater. 337–339 (2005) 17.